Available online at www.sciencedirect.com
SCIENCE DIRECT
Trans. Nonferrous Met. Soc. China 18(2008) 346−350
Transactions of Nonferrous Metals Society of China
www.csu.edu.cn/ysxb/

Preparation of $NaV_{1-x}Al_xPO_4F$ cathode materials for application of sodium-ion battery

LIU Zhi-ming(刘志明)[1], WANG Xian-you(王先友)[1], WANG Ying(王 莹)[2], TANG An-ping(唐安平)[1], YANG Shun-yi(杨顺毅)[1], HE Liang-fu(何亮甫)[1]

1. School of Chemistry, Xiangtan University, Xiangtan 411105, China;
2. School of Chemical Engineering and Pharmacy, Wuhan Institute of Technology, Wuhan 430073, China

Received 1 June 2007; accepted 29 August 2007

Abstract: The effects of Al doping on the electrochemical properties of $NaVPO_4F$ as a cathode material for sodium-ion batteries were investigated. Al-doped $NaV_{1-x}Al_xPO_4F$ (x=0, 0.02) samples were prepared by a simple high temperature solid-state reaction involving VPO_4 and NaF for the application of cathode material of sodium-ion batteries. The crystal structure and morphology of the material were studied by Flourier-infrared spectrometry(FT-IR), X-ray diffractometry(XRD) and scanning electron microscopy(SEM). The results show that $NaV_{1-x}Al_xPO_4F$ (x=0, 0.02) has a typical monoclinic structure. The effects of Al doping on the performance of the cathode material were analyzed in terms of the crystal structure, charge-discharge curves and cycle performance. It is found that $NaV_{0.98}Al_{0.02}PO_4F$ shows an improved cathodic behavior and discharge capacity retention compared with the undoped samples in the voltage range of 3.0−4.5 V. The electrodes prepared from $NaV_{0.98}Al_{0.02}PO_4F$ deliver an initial discharge capacity of 80.4 mA·h/g and an initial coulombic efficiency of 89.2%, and the capacity retention is 85% after 30th cycle. Though the Al-doped samples have lower initial capacities, they show better cycle performance than Al-free samples.

Key words: sodium ion battery; cathode materials; capacity retention; cycle performance

1 Introduction

Lithium-ion batteries have become attractive energy storage systems for portable electronic devices as they offer higher energy density compared with the other rechargeable systems. If rechargeable sodium-ion batteries with good electrochemical performance could be developed, it would have some advantages over lithium-ion batteries, such as a lower raw materials cost and the ability to utilize electrolyte systems of lower decomposition potential (due to the higher half-reaction potential for sodium relative to lithium, $\varphi^0_{Na^+/Na} = \varphi^0_{Li^+/Li} + 0.3\,V$) [1], so sodium-ion batteries are safer than the lithium-ion batteries. Therefore, sodium-ion batteries will be a kind of prospective novel batteries.

The anode materials in sodium-ion batteries have currently made a great progress[2−6], thus the key of sodium-ion batteries development is the preparation of cathode materials with good electrochemical performance. Up to now, several cathode materials have been reported, for example, Na_xTiS_2, $Na_xNbS_2Cl_2$, Na_xWO_{3-x}, $Na_xV_{0.5}Cr_{0.5}S$, Na_xMoS_3, Na_xTaS_2 and $Na_3V_2(PO_4)_2F_3$[6−10]. However, the bad electrochemical performances prevent these materials to be further used.

Recently, BARKER et al[11] reported a novel sodium-ion battery that based on a hard carbon/$NaVPO_4F$ chemistry. The average discharge voltage for the sodium-ion cells was demonstrated to be around 3.7 V, comparable with commercially available lithium-ion cells. The reversible specific capacities for the cathode and anode active materials were determined to be 82 and 202 mA·h/g, respectively. Representative test cells cycled more than 30 times before their discharge capacity had declined to less than 50% of the original one. Although $NaVPO_4F$ is now considered a hopeful cathode material for sodium-ion battery, its electrochemical performance should be improved. It is well known that doping technology has been widely used in lithium-ion battery to improve the

Foundation item: Project(50472080) supported by the National Natural Science Foundation of China; Projects(04JJ3040, 05JJ20013) supported by the Natural Science Foundation of Hunan Province, China; Project(BK2003092) supported by the Natural Science Foundation of Jiangsu Province, China
Corresponding author: WANG Xian-you; Tel: +86-732-8293043; Fax: +86-732-8292282; E-mail: wxianyou@yahoo.com

capacity retention, for example, Al doped or Cr doped cathode materials have better cycleability than pure cathode materials[12−15]. In this work, $NaVPO_4F$ was synthesized by a high temperature solid-state reaction, and Al was doped into this material to prepare $NaV_{1-x}Al_xPO_4F$ (x=0, 0.02) powders. The effects of Al doping on the structure and electrochemical properties of $NaV_{1-x}Al_xPO_4F$ were discussed based on FT-IR, XRD, SEM, CV, charge-discharge curves and cycle performance.

2 Experimental

$NaV_{1-x}Al_xPO_4F$ (x=0, 0.02) was prepared with a high temperature solid-state reaction, using VPO_4 as a reaction intermediate. A proprietary carbon thermal reduction(CTR) method[11] involving V_2O_5, $NH_4H_2PO_4$ and C was used to make the VPO_4 precursor. The incorporation reaction may be summarized as

$$1/2V_2O_5+NH_4H_2PO_4+C\rightarrow VPO_4+NH_3+3/2H_2O+CO \quad (1)$$

Stoichiometric reactants were intimately mixed and then pelletized. In order to complete vanadium reduction, 25% excess carbon was used based on reaction (1). The mixture was heated to 750 ℃, and held for 4 h inside a temperature-controlled tube furnace.

Then, the stoichiometric amounts of $Al(OH)_3$ and $NH_4H_2PO_4$ were mixed and then pelletized. The pellets were initially heated to 950 ℃ for 8 h in the air. The incorporation reaction may be summarized as

$$Al(OH)_3+NH_4H_2PO_4\rightarrow AlPO_4+NH_3+3H_2O \quad (2)$$

In the finally stage of preparation, VPO_4 and $AlPO_4$ were reacted with the alkali fluoride to make the products $NaV_{1-x}Al_xPO_4F$:

$$NaF+(1-x)VPO_4+xAlPO_4\rightarrow NaV_{1-x}Al_xPO_4F \quad (3)$$

Infrared spectra were recorded on Fourier transform infrared(FTIR) spectrometer (Perkin-Elmer Spectrum one) in the wavelength range from 4 000 to 500 cm^{-1}, using the KBr disk method. Powder X-ray diffraction (D/max-2550 Rigaku, Japan) measurement using Cu K_α radiation was employed to identify the crystal structure of products. The morphology and particle sizes of products were examined via scanning electron microscope(SEM) using a JEOL Microscope.

The positive electrodes were fabricated by mixing $NaV_{1-x}Al_xPO_4F$ powders with carbon black and PTFE binder in the mass ratio of 75:15:10. The mixture was pressed onto stainless steel mesh used as current collector and dried under vacuum at 120 ℃ for 24 h. The laboratory cells consisted of the cathode, the sodium foils as an anode and 1 mol/L $NaClO_4$-EC/DMC (1:1 in volume) as an electrolyte were assembled in an argon-filled glove box. Electrochemical tests were performed between 3.0 and 4.5 V with a rate of 0.1C at 25 ℃ with a BTS-51800 Neware Battery Testing System (Shenzhen, China).

3 Results and discussion

Fig.1 shows the FT-IR spectra of $NaV_{1-x}Al_xPO_4F$ (x=0, 0.02). The analysis of the spectrum was carried out in the area of PO_4^{3-} group oscillations. It can be seen from Fig.1 that there are no obvious changes in stretching vibration band with the Al doping. The broad band in 1 051 cm^{-1} is assigned to the absorbed peak resulted by PO_4^{3-} anions asymmetric stretching, and it becomes narrow. In addition, the symmetric stretching vibrations, ν_s (PO_4), appear in the 690−630 cm^{-1} range. The bands corresponding to the asymmetric deformation of the PO_4^{3-} anions are located in 540−580 cm^{-1}. FT-IR measurements show the existence of the type of PO_4^{3-} tetrahedral in the structure. Moreover, it is found that the band peak moves to higher band direction as the Al is doped. So, it explains that the strength of V—O band increases with the doped Al and the crystal cell shrinks. Thus it can be expected that the stability of materials will be enhanced and the cycle performance will be better with the introduction of Al.

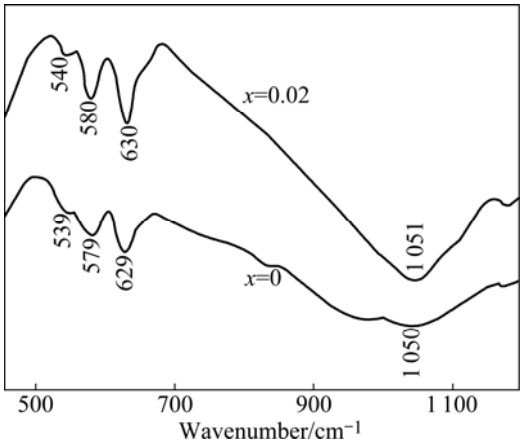

Fig.1 FT-IR spectra of $NaV_{1-x}Al_xPO_4F$ (x=0, 0.02)

Fig.2 shows the X-ray diffraction patterns of the $NaV_{1-x}Al_xPO_4F$ (x=0, 0.02) powders prepared by high temperature solid-state reaction. The crystal phases of both samples are identified to be a monoclinic structure (space group: $C2/c$) according to the standard card (PDF33-0804). No impurities are detected from the XRD results. The proposed structure is also in good accordance with the structural analysis of the related compound, $Na_3Al_2(PO_4)_2F_3$[16]. That is, the aluminum compound demonstrates facile sodium-ion diffusion (as

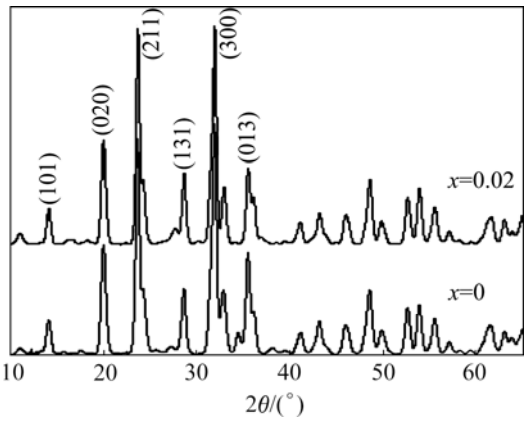

Fig.2 XRD patterns of $NaV_{1-x}Al_xPO_4F$ (x=0, 0.02)

evidenced by ionic conductivity measurements) through an extended three-dimensional framework built up from two different [AlO_4F_2] octahedrons and two [PO_4] tetrahedrons. This structure produces cavities, in which the sodium ions are statistically distributed. To research the influence of the Al doping on the structure, Rietveld refinements were carried out for all compositions and the calculated lattice parameters are listed in Table 1. By comparing the Al-free powder, it is observed from Fig.2 and Table 1 that the diffraction peaks are shifted to a higher angle, which indicates a gradual decrease in lattice parameters. The reason for the decrease of its structural parameter in Table 2 is primarily due to the difference in the ionic radius of Al^{3+} (0.053 5 nm) and V^{3+} (0.064 0 nm). The substitution of V^{3+} with Al^{3+} results in the shrinkage of the unit cell volume. In addition, the bonding energy of Al—O (512 kJ/mol) is higher than that of the V—O (485 kJ/mol) bond, which enhances the stability of the monoclinic structure during insertion and deinsertion of sodium ion, and decreases the capacity loss of the battery after 30 cycles.

Scanning electron microscopy(SEM) images of the $NaV_{1-x}Al_xPO_4F$ (x=0, 0.02) powder are shown in Fig.3. It is observed that an amount of primary particles conglomerate the secondary particles, and the average particle size of the sample is about 8−10 μm; in addition, some cubic shape particles can be found in all of these samples. Compared with the Al-free sample, $NaV_{0.98}Al_{0.02}PO_4F$ has a smaller particle size, which also suggests that Al is well permeated into the bare $NaVPO_4F$ forming a solid solution. The electrochemical performance of the $NaV_{1-x}Al_xPO_4F$ (x=0, 0.02) is known to be good because the insertion and de-insertion of Na^+ during the charge and discharge processes can be facilitated when electrode materials are smaller in size[16].

Fig.4 shows the cyclic voltammograms of $NaVPO_4F$ and $NaV_{0.98}Al_{0.02}PO_4F$ at 0.15 mV/s in the potential range of 3.0−4.5 V. It can be seen from Fig.4 that $NaVPO_4F$ samples have two pairs of redox current peaks at about 3.61 V/3.72 V and 3.99 V/4.40 V, respectively; while $NaV_{0.98}Al_{0.02}PO_4F$ samples have two pairs of redox current peaks at about 3.69 V/3.83 V and

Table 1 Lattice parameters for $NaV_{1-x}Al_xPO_4F$

Sample	x(Al)	a/nm	b/nm	c/nm	α/(°)	β/(°)	γ/(°)
$NaV_{0.98}Al_{0.02}PO_4F$	0.00	0.887	0.874	0.757	90.00	124.35	90.00
$NaVPO_4F$	0.02	0.849	1.229	0.647	90.00	105.19	90.00

Table 2 Charge-discharge capacity and capacity retention ratio of samples

Cathode material	First charge capacity/ ($mA\cdot h\cdot g^{-1}$)	First discharge capacity/ ($mA\cdot h\cdot g^{-1}$)	Capacity loss in first cycle/ ($mA\cdot h\cdot g^{-1}$)	Reversible efficiency in first cycle/%	Discharge capacity at 30th cycle/ ($mA\cdot h\cdot g^{-1}$)	Capacity retention ratio at 30th cycle/%
$NaVPO_4F$	102.5	86.3	16.2	84.2	50.4	58.4
$NaV_{0.98}Al_{0.02}PO_4F$	90.1	80.4	9.7	89.2	68.3	85.0

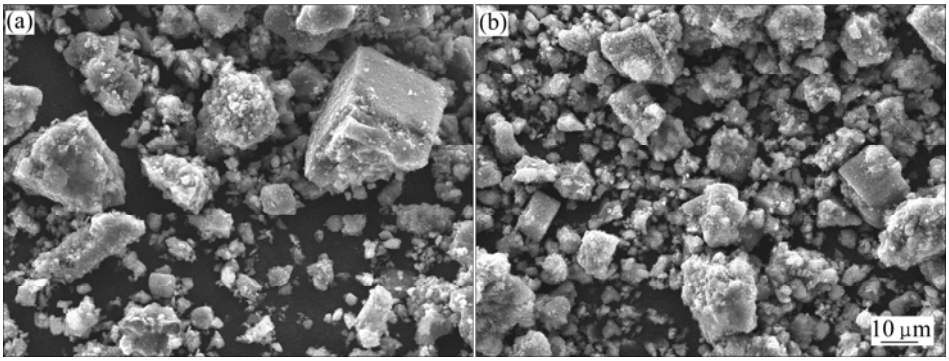

Fig.3 SEM micrographs of $NaV_{1-x}Al_xPO_4F$: (a) x=0; (b) x=0.02

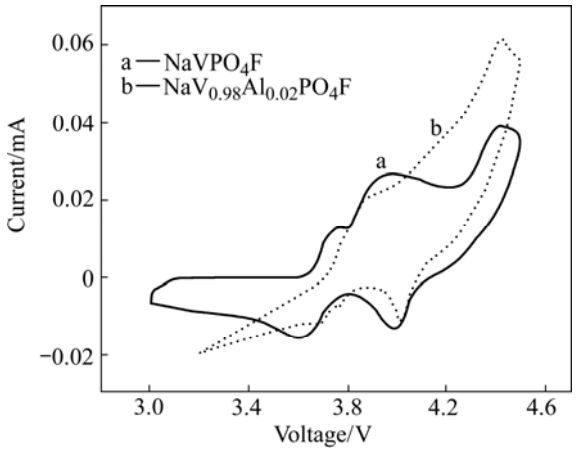

Fig.4 Cyclic voltammograms of NaVPO4F and $NaV_{0.98}Al_{0.02}PO_4F$ with 0.15 mV/s at 3.0−4.5 V

4.01 V/4.42 V, respectively. These two pairs of redox peaks correspond to the intercalation and deintercalation of sodium-ion in the $NaVPO_4F$ and $NaV_{0.98}Al_{0.02}PO_4F$, respectively. Besides, the potentials of redox current peak shift toward more positive. Therefore, during the oxidation process, it is found that the $NaV_{0.98}Al_{0.02}PO_4F$ sample has higher oxidation potential than $NaVPO_4F$ sample corresponding to the extraction of Na^+ ions. Deintercalation of Na^+ ions at higher potential indicates that more driving force is necessary to impel the Na^+ from the host structure to the anode. This implies that the $NaV_{0.98}Al_{0.02}PO_4F$ sample has better reversibility.

In order to further study the influence of Al doping on the electrochemical performance, the cells were operated at a charge/discharge current density of 10 mA/g at ambient temperature. Fig.5 shows the initial charge/discharge curves of the $NaV_{1-x}Al_xPO_4F$ (x=0, 0.02) powder. Charge-discharge capacity and capacity retention ratio of the samples are listed in Table 2. As seen from Fig.5 and Table 2, all cells show quite smooth and monotonous charge/discharge curves. The Al-free

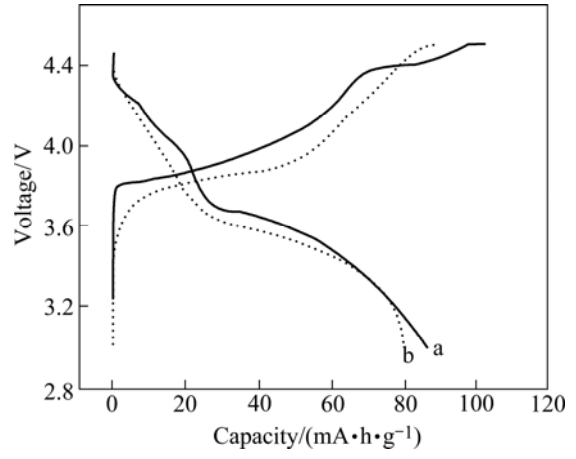

Fig.5 First charge-discharge curves of $NaV_{1-x}Al_xPO_4F$: (a) x=0; (b) x=0.02

sample has the initial discharge capacity of 86.3 mA·h/g, showing a coulombic efficiency of 84.2%. However, the $NaV_{0.98}Al_{0.02}PO_4F$ delivers a slightly decreased discharge capacity of 80.4 A·h/g, of which the efficiency corresponds to 89.2%. The initial reversible capacity decreases by the Al doping, but the efficiency is enhanced.

Fig.6 shows the changes of discharge capacity of the $NaV_{1-x}Al_xPO_4F$ (x=0, 0.02) powder for different contents of Al with cycle number. Although the Al-free $NaV_{1-x}Al_xPO_4F$ (x=0) electrodes have the higher initial discharge capacity, they show abrupt decrease in capacity during cycling and the capacity retention is 58.4% at the 30th cycle, while the Al-doped samples $NaV_{0.98}Al_{0.02}PO_4F$ show obviously improved cycle performance though they have slightly lower initial discharge capacity. The $NaV_{0.98}Al_{0.02}PO_4F$ has a discharge capacity of 80.4 mA·h/g, and the capacity retention is 85% at the 30th cycle, however BARKER et al[11] reported that the capacity retention of $NaVPO_4F$ as cathode material is only 50% at the 30th cycle. Moreover, it can be seen that after 10 cycles, the obtained discharge capacity of $NaV_{0.98}Al_{0.02}PO_4F$ is even higher than that of the Al-free sample. From these results, Al doping of $NaVPO_4F$ is an effective means to substantially enhance cycleability during cycling, and $NaV_{0.98}Al_{0.02}PO_4F$ has good electrochemical performance for the application of sodium ion batteries.

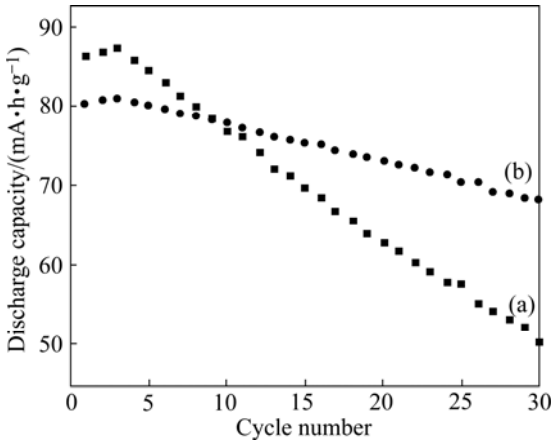

Fig.6 Plots of specific discharge capacity vs cycle numbers of $NaV_{1-x}Al_xPO_4F$: (a) x=0; (b) x=0.02

4 Conclusions

1) $NaV_{1-x}Al_xPO_4F$ (x=0, 0.02) materials were successfully synthesized by high temperature solid-state reaction. All samples have a monoclinic structure and no impurities.

2) The particle size of $NaV_{0.98}Al_{0.02}PO_4F$ is smaller than that of the Al-free sample. The $NaV_{0.98}Al_{0.02}PO_4F$ materials show good electrochemical performance. The

Al-doped sample shows better cycle performance compared with the Al-free sample. The $NaV_{0.98}Al_{0.02}PO_4F$ electrode delivers an initial discharge capacity of 80.4 mA·h/g between 3 and 4.5 V with a current density of 10 mA/g at ambient temperature, and the capacity retention at the 30th cycle is 85%. The outstanding electrochemical properties of $NaV_{0.98}Al_{0.02}PO_4F$ make it a promising cathode material for sodium-ion batteries.

References

[1] STEVENS D A, DAHN J R. High capacity anode materials for rechargeable sodium-ion batteries [J]. J Electrochem Soc, 2000, 147: 1271−1274.

[2] BACH S, MILLET M, PERIERA-RAMOS M J P, SANCHEZ L, LAVELA P, TIRADO J L. Electrochemical sodium insertion into MnCo oxide [J]. Electrochem Solid-State Lett, 1999, 2(11): 545−546.

[3] DOEFF M M, MA Y, VISCO S J, DEJONGHE L C. Electrochemical insertion of sodium into carbon [J]. J Electrochem Soc, 1993, 140: L169−L170.

[4] THOMAS P, GHANBAJA J, BILLAUD D. Electrochemical insertion of sodium in pitch-based carbon fibres in comparison with graphite in $NaClO_4$-ethylene carbonate electrolyte [J]. Electrochem Acta, 1999, 45: 423−428.

[5] UEBOU Y, OKADA S, YAMAKI J. Electrochemical insertion of lithium and sodium into $(MoO_2)_2P_2O_7$ [J]. J Power Sources, 2003, 115: 119−124.

[6] DOEFF M M, RICHARDSON T J, HOLLINGSWORTH J, YUAN C W, GOZALES M. Synthesis and characterization of a copper-substitute manganese oxide with the Na0.44MnO2 [J]. J Power Sources, 2002, 112: 294−297.

[7] WU Zhen-jun, CHEN Zong-zhang, TANG Hong-wei, LI Su-fang. The research progress of sodium-ion battery [J]. Battery Bimonthly, 2002, 32: 45−47. (in Chinese)

[8] WEST K, ZACHAU-CHRISTIANSEN B, JACOBSEN T. Sodium insertion in vanadium oxides [J]. Solid-State Ionics, 1988, 28/30: 1128−1131.

[9] DOEFF M M, FERRY Y, MA Y, DING L, DEJONGHE L C. Effect of electrolyte composition on the performance of sodium/polymer cells [J]. J Electrochem Soc, 1997, 144: L20−L22.

[10] BARKER J, GOVER R K B, BURNS P, BRYAN A J. Hybrid lithium-ion cell based on a sodium insertion material [J]. Electrochem Journal of Solid State Chemistry, 2006, 9(4): A190−A192.

[11] BARKER J, SAIDI M Y, SWOYER J L. A sodium-ion cell based on the fluorophosphates compound $NaVPO_4F$ [J]. Electrochem Solid-State Lett, 2003, 6: A1−A4.

[12] PARK S H, SUN Y K. Synthesis and electrochemical properties of layered $Li[Li_{0.15}Ni_{(0.275-x/2)}Al_xMn_{(0.575-x/2)}]O_2$ materials prepared by sol-gel method [J]. J Power Sources, 2003, 119/121:161−165.

[13] BAO Shu-juan, LIANG Yan-yu, ZHOU Wen-jia, HE Ben-lin, LI Hu-lin. Synthesis and electrochemical properties of $LiAl_{0.1}Mn_{1.9}O_4$ by microwave-assisted sol-gel method [J]. J Power Sources, 2006, 154(1): 239−245.

[14] YING Jie-rong, LEI Min, JIANG Chang-yin, WAN Chun-rong, HE Xiang-ming, LI Jian-jun, WANG Li, REN Jian-guo. Preparation and characterization of high-density spherical $Li_{0.97}Cr_{0.01}FePO_4$/C cathode material for lithium ion batteries [J]. J Power Sources, 2006, 158(1): 543−549.

[15] YI Ting-feng, HU Xin-guo, GAO Kun. Synthesis and physicochemical properties of $LiAl_{0.05}Mn_{1.95}O_4$ cathode material by the ultrasonic-assisted sol-gel method [J]. J Power Sources, 2006, 162(1): 636−643.

[16] LE MEINS J M, CROSNIER-LOPEZ M P, HEMON-RIBAUD A, COURBION G. Phase transitions in the $Na_3M_2(PO_4)_2F_3$ family ($M=Al^{3+}$, V^{3+}, Cr^{3+}, Fe^{3+}, Ga^{3+}): Synthesis, thermal, structural, and magnetic studies [J]. J Solid-State Chem, 1999, 148: 260−277.

(Edited by LI Xiang-qun)